Available online at www.sciencedirect.com
ScienceDirect
Progress in Natural Science: Materials International 21(2011) 240−245
Progress in Natural Science: Materials International
www.elsevier.com/locate/pnsc

Effects of hydrogen on a tungsten grain boundary: A first-principles computational tensile test

Hong-bo ZHOU, Shuo JIN, Ying ZHANG, Guang-hong LU

Department of Physics, Key Laboratory of Micro-nano Measurement-Manipulation and Physics (Ministry of Education), Beijing University of Aeronautics and Astronautics, Beijing 100191, China

Received 21 February 2011; accepted 13 May 2011

Abstract: A first-principles computational tensile test has been preformed to investigate the effects of hydrogen on a tungsten grain boundary. It has been found that the maximum ideal tensile strength of the tungsten grain boundary with hydrogen atom segregation was 32.85 GPa, which was about 9% lower than that of the clean tungsten grain boundary (36.23 GPa). This indicated that the theoretical strength of the tungsten grain boundary became weaker in the presence of the hydrogen atom. Atomic configuration analysis showed that the grain boundary fracture was caused by the interfacial bond breaking. The Griffith fracture energy was calculated to be 161 meV/Å^2 (2.58 J/m^2) and 155 meV/Å^2 (2.48 J/m^2) for the tungsten grain boundary without and with the hydrogen atom segregation, respectively. The solution energy of the hydrogen atom in a fracture free surface was −0.31 eV, which was 0.08 eV lower than that of the hydrogen atom in a tungsten grain boundary. This indicated that hydrogen was a grain boundary embrittler according to the Rice-Wang thermodynamic theory. The Bader charge analysis suggested that the physical origin for hydrogen-induced embrittlement was the charge transfer induced by hydrogen in the tungsten grain boundary.
Key words: tungsten; hydrogen; grain boundary; tensile strength; first-principles

1 Introduction

Nowadays, energy shortage drives us to pay great efforts to developing nuclear fusion and thereby it is going to be of practical use in the foreseeable future. The final application of nuclear fusion energy is mainly dependent on the development of key materials in the thermonuclear fusion device Tokamak, in which the choice of the plasma facing material (PFM) is one of the key issues. Tungsten and tungsten alloys are the most promising candidates for PFM including both first wall and divertor plate in Tokamak because of their good thermal properties such as high thermal conductivity, high melting temperature and low sputtering erosion [1]. However, as a PFM, tungsten will be exposed to extremely high fluxes of hydrogen isotope ions. It must not only withstand radiation damage, but also keep intrinsic mechanical properties. Therefore, the relationship between the microstructures and mechanical properties of tungsten under hydrogen irradiation is one of the key concerns for its use in fusion reactor, and has been under intensive investigations [2−8].

Generally, defects in materials, such as grain boundaries, dislocations, and vacancies, are considered to play crucial roles in various properties of materials. The role of the grain boundaries gets much more attention among them. For example, the grain boundary brittleness has been considered to be a fatal factor to seriously limit Ni_3Al application [9]. The grain boundary acts as a transition region between two adjacent crystal lattices, and thus the chemical composition and crystallographic structure of the grain boundaries are distinct from those of the bulk crystal. Therefore, such distinct composition and structure powerfully affect the chemical and physical behaviors of the grain boundaries, and the properties of materials with the grain boundaries can greatly differ from those of a single crystal [10]. Some elements will segregate to the grain boundaries due to different chemical composition between the grain boundaries and the surrounding bulk [11]. Recently, with the aid of high performance supercomputers and sophisticated quantum mechanical method, the first-principles calculations based on density-functional theory have been successfully applied to investigating the embrittlement induced by impurities segregating in the grain boundaries [12−14].

Previous investigations [15−19] showed that the bombardment of high flux of hydrogen isotope ions could cause roughening and blistering in tungsten and

Corresponding author: Shuo JIN; E-mail: jinshuo@buaa.edu.cn

suggested that the tungsten grain boundary played an important role in the formation of hydrogen bubbles. The hydrogen bubbles would be the most possibly to form along the tungsten grain boundaries [15]. The implanted hydrogen would diffuse further into the material, which could eventually find trapping sites in the grain boundaries and collect [16−17], leading to the nucleation and growth of hydrogen bubbles [18−19]. Furthermore, the formation of hydrogen bubbles (blisters) would reduce grain boundary adhesion [19].

Detailed descriptions of the hydrogen atom in the tungsten grain boundary have become attainable based on the recent advances in first-principles theory and computing power. The grain boundaries in tungsten served as trapping center for hydrogen [5]. It has been demonstrated that hydrogen could be easily trapped by the tungsten grain boundaries with the solution and segregation energies of −0.23 eV and −1.11 eV, respectively. Kinetically, such trapping was easier to be realized due to the much lower diffusion barrier of 0.13−0.16 eV from the bulk to the grain boundary in comparison with the segregation energy, suggesting that the trapped hydrogen was quite difficult to escape out of the grain boundary. However, the effect of hydrogen on the tensile strength of the tungsten grain boundary systems has not been explored so far. By a first-principles computational tensile test (FPCTT), the ideal tensile strength of the grain boundary can be determined by the first-principles method [12−14, 20−22]. In this paper, using the FPCTT, the ideal tensile strength of a tungsten grain boundary with the segregated hydrogen atoms has been investigated. This could help us to further understand the effect of hydrogen on the tungsten grain boundary.

2 Computational methods

Our first-principles calculations were performed using the pseudopotential plane-wave method implemented in the VASP code [23−24] based on the density functional theory. The generalized gradient approximation of PERDEW and WANG [25] and projected augmented wave potentials [26] were used, with a plane wave energy cutoff of 350 eV. The supercell contained 80 tungsten atoms to simulate the 36.9° [100]{013}∑=5 symmetrical tilt grain boundary, as shown in Fig. 1. The calculated equilibrium lattice constant was 3.17 Å for body-center cubic tungsten, which was in good agreement with the corresponding experimental value of 3.16 Å [27]. The dimensions of the tungsten grain boundary supercell were 20.87 Å× 9.97 Å×6.29 Å. For summation over Brillouin zone, the

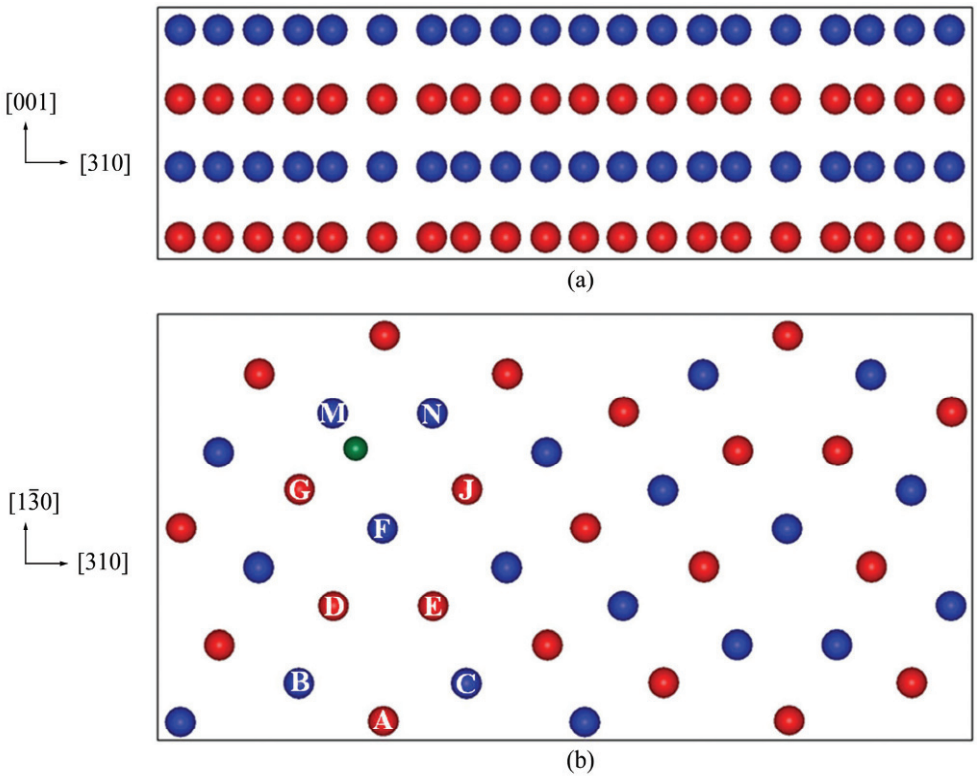

Fig. 1 Side view of ∑5(310)/[001] tilt tungsten grain boundary (a) and top view of tungsten grain boundary supercell (b) (Schematically, the larger blue and red spheres corresponded to the different layers in the supercell, while the smaller green sphere represented for the hydrogen atom. Tungsten atoms were denoted by *A*-*N* for later discussions.)

uniform grids of *k*-points were 1×2×3 according to the Monkhorst-Pack scheme with a full relaxation of the atomic positions and volume of the supercell [28]. The hydrogen atom occupied the most stable site in the tungsten grain boundary shown in previous study [5]. The tensile strength of the bulk tungsten in the [310] direction was also calculated in order to compare with the clean grain boundary. The energy relaxation iterates until the forces acting on all the atoms were less than 10^{-3} eV/Å.

In the tensile test, the Hellmann-Feynman theorem was adopted to determine the tensile stress through the Nielsen-Martin scheme [29], according to which the stress $\sigma_{\alpha\beta}$ could be calculated from

$$\sigma_{\alpha\beta} = \frac{1}{\Omega}\frac{\partial E_{\text{total}}}{\partial \varepsilon_{\alpha\beta}} \quad (1)$$

where E_{total} was the total energy of the tungsten grain boundary with strain, $\sigma_{\alpha\beta}$ is the strain tensor (α, β=1, 2, 3), and Ω is the volume of the unit cell. A uniaxial tensile strain was introduced in the grain boundary normal direction [310]. The lattice dimensions in the grain boundary plane were fixed to simplify the calculation, without considering Poisson's ratio. In each strain step, the starting atomic configuration was taken by uniform scaling from the fully relaxed configuration of the preceding step to ensure the continuous strain path. More calculation details could be found elsewhere [30].

3 Results and discussion

3.1 FPCTT of clean tungsten grain boundary

Figure 2 showed the tensile stress as a function of strain in the [310] direction. It could be observed that for the bulk system, the tensile stress increased with increasing tensile strain until a strain of 24%, at which the stress reached a maximum, as shown in Fig. 2. After a strain of 24%, the stress decreased gradually. Hence, the maximum stress of 46.41 GPa was the theoretical tensile strength of the bulk tungsten in the [310] direction. For the clean grain boundary system, Figure 2 demonstrated that the stress increased initially with increasing strain, and exhibited a maximum stress of 36.23 GPa at a strain of 14%. The stress decreased quickly when the strain was larger than 14%. Therefore, the maximum ideal tensile strength of the clean grain boundary was 36.23 GPa in the [310] direction, which was 22% lower than that of the bulk tungsten. This indicated that the theoretical strength of tungsten became weaker in the presence of the grain boundary.

In order to understand the tensile strength decrease due to the grain boundary, the interfacial bond lengths of the grain boundary were investigated. Figure 3(a) displayed the calculated binding energy between two

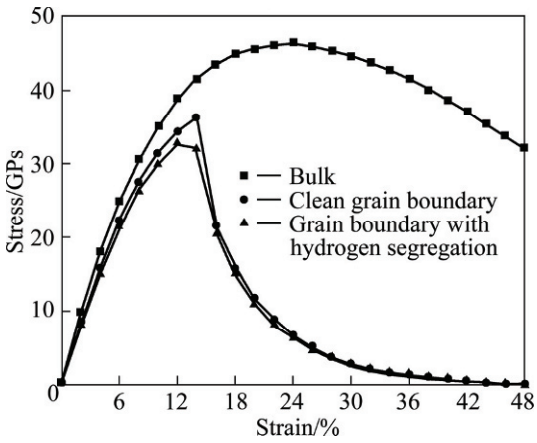

Fig. 2 Stress of bulk tungsten, clean grain boundary, and hydrogen atom-segregated grain boundary as function of strain in grain boundary normal direction

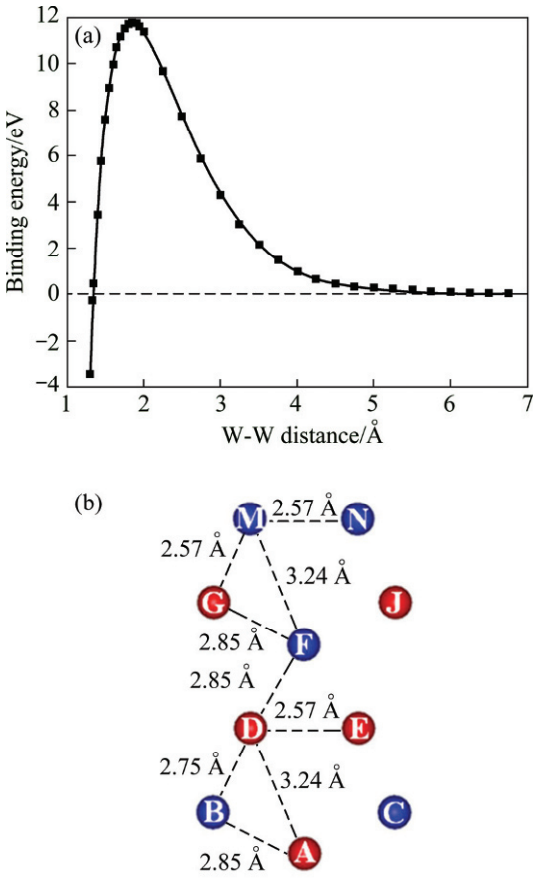

Fig. 3 Calculated binding energy (eV) of a W-W pair in vacuum as a function of W-W spatial separation (Positive values indicated attraction, while negative ones indicated repulsion) (a) and atomic configurations surrounding grain boundary plane (b)

tungsten atoms as a function of the tungsten-tungsten (W-W) interatomic distance in vacuum. It showed a repulsive interaction between tungsten atoms when their interatomic distance was lower than 1.33 Å. Beyond this distance, the binding energy increased rapidly with the

increase of the W-W interatomic distance. It experienced a peak at a W-W equilibrium distance of about 1.85 Å with the largest binding energy of 11.73 eV. After this, the binding energy decreased rapidly and converged to zero, as shown in Fig. 3(a). In the bulk tungsten, the distance between the nearest neighbor tungsten atoms was 2.74 Å, which indicated that there was strong attraction between tungsten atoms in the bulk tungsten.

In the clean grain boundary case, the interfacial bond lengths were calculated to be in the range of 2.57−3.24 Å, as illustrated in Fig.3(b). It could be found that the bond lengths for *BD* (*GM*), *AB* (*DF* and *FG*), and *AD* (*FM*) were longer than that of the W-W bond in the bulk tungsten by 0.03 Å, 0.11 Å, and 0.50 Å, respectively. Only the *DE* (*MN*) with bond length of 2.57 Å was shorter than that of the W-W bond in the bulk tungsten. This suggested that the most of interfacial bonds of the grain boundary became weaker in comparison with the W-W in the bulk tungsten, which should be responsible for the decrease of the grain boundary theoretical strength.

3.2 FPCTT of tungsten grain boundary with hydrogen segregation

In the previous study [5], it has been demonstrated that the tungsten grain boundary could serve as a trapping center for hydrogen due to the strong binding between hydrogen and the grain boundary. Hydrogen atom could easily segregate into a tungsten grain boundary with the segregation energy of −1.11 eV, which was shown to be low enough for the trapping of almost all hydrogen atoms into the grain boundary, independent of the temperature (300−900 K) and the bulk hydrogen atoms concentration (500−1 000 appm). Through performing the FPCTT, the ideal tensile strength and the Griffith fracture energy could be determined for the clean grain boundary and the hydrogen atom-segregated grain boundary, respectively. These quantities could help us to theoretically understand how the mechanical properties of the tungsten grain boundary change due to the hydrogen atom segregation.

The tensile stress of the hydrogen atom-segregated grain boundary as a function of strain is illustrated in Fig. 2. The stress reached its maximum of 32.85 GPa at a strain of 12% after a continuous increase with increasing strain. Beyond the strain of 14%, the stress dropped suddenly to 20.54 GPa, and approached slowly to zero. The ideal tensile strength of the hydrogen atom-segregated grain boundary was 32.85 GPa. In comparison with the clean grain boundary, the tensile strength was reduced by about 9% due to the hydrogen atom segregation.

The Griffith fracture energy was defined as the requisite energy to create unit crack surface. As shown in Fig. 2, the stress was zero at the strain of 48%. This indicated that the grain boundary turned into free crack surface after the strain of 48%, and thus the Griffith fracture energy was directly associated with the energy difference between the grain boundary with strain of 48% and without strain. The energy difference was calculated to be 40.42 eV for the clean grain boundary and 39.08 eV for the hydrogen atom-segregated grain boundary, corresponding to the Griffith fracture energy of 161 meV/Å^2 (2.58 J/m^2) and 155 meV/Å^2 (2.48 J/m^2), respectively. The fracture energy of the hydrogen atom-segregated grain boundary was about 4% lower than that of the clean grain boundary. Thus, theoretical crack in tungsten with the grain boundary segregation of hydrogen would be easier to extend according to the Griffith energy criterion of fracture.

The fracture mode of solid also could be determined by the competition between plastic crack blunting and brittle boundary separation based on a thermodynamic theory described by RICE and WANG [31]. The potency of a segregation impurity in reducing the "Griffith work" of brittle boundary separation was a linear function of the difference in solution energies for impurity at the grain boundary and the free surface (FS). Therefore, whether hydrogen was an embrittler in a tungsten grain boundary could be determined by estimating the solution energy difference of a hydrogen atom in a grain boundary (E_{GB}^{sol}) and a fracture-FS (E_{FS}^{sol}). As mentioned above, the solution energy of the hydrogen atom in a tungsten grain boundary was −0.23 eV. After the grain boundary fracture (strain of 48%), the solution energy of the hydrogen atom in a fracture-FS was calculated to be −0.31 eV in reference to the clean fracture-FS and half the energy of the hydrogen molecule [5]. $E_{FS}^{\mathrm{sol}} - E_{GB}^{\mathrm{sol}}$ was calculated to be -0.08 eV, which was negative, indicating that hydrogen was a grain boundary embrittler according to the Rice-Wang thermodynamic theory.

Thus, it was clear that the tensile strength of the tungsten grain boundary was reduced by about 9% due to the hydrogen atom segregation, and the Griffith fracture energy was reduced by about 4%. Consequently, the hydrogen atom-segregated grain boundary was easier to break under applied stress as compared with the clean one.

3.3 Charge transfer induced by hydrogen segregation

In order to explore the hydrogen-induced embrittlement of the tungsten grain boundary, the charge transfer between hydrogen and tungsten atoms has been investigated. A quantitative analysis of electron density was performed following the prescriptions of Bader's theory of atoms in molecules [32−33]. In this calculation, based on the charge density distribution, the real-space was partitioned into several subspaces associated with

each atom. The boundary of an atom was delimited by the zero-flux surface of the charge density gradient vector field on which the charge density reaches the minimum perpendicular to the surface. The integrated charge enclosed within the zero-flux surfaces could be taken as a good approximation of the charge of an atom.

Table 1 Calculated Bader charges (in the unit of e) for hydrogen atom and five neighboring tungsten atoms and corresponding distances between hydrogen and tungsten $d_{H–W}$ in unit of Å

Site	Bader charge/e	$d_{H–W}$/Å
H	−0.61	−
W(*F*)	+0.12	1.98
W(*G*)	+0.18	1.97
W(*J*)	+0.07	2.45
W(*M*)	+0.05	2.62
W(*N*)	+0.01	2.85

As shown in Fig. 1, there were five neighboring tungsten atoms (*F*, *G*, *J*, *M*, and *N*) for hydrogen in the grain boundary. Table 1 presents the Bader charges of both the hydrogen atom and the neighboring tungsten atoms. The hydrogen atom obtained the electron from the host tungsten and became negative charged, with the Bader charge of −0.61 e. The Bader charges were +0.12 e and +0.18 e for the first nearest neighbour tungsten atoms (*F* and *G*), respectively, with the shorter distance of about 1.97 Å from the hydrogen atom. For the second nearest neighboring tungsten atoms (*J* and *M*), the Bader charges were around +0.06 e. For the tungsten atom(*N*) with a farther distance from the hydrogen atom (2.85 Å), the Bader charge decreased to almost zero. This indicated that the Bader charge of tungsten atoms was directly associated with the distance from the hydrogen atom.

The Bader charge results suggested the presence of the hydrogen atom leading to the charge density redistribution of host atoms in the tungsten grain boundary. The hydrogen atom acted as an electron acceptor in the tungsten grain boundary, which got electron from tungsten atoms, leading to a decrease of tungsten valence electron. For example, the valence electrons of tungsten atoms (*F* and *G*) were 5.85e and 6.01e in the clean tungsten grain boundary, respectively, while it decreased to be 5.73e and 5.83e with the segregated hydrogen atom. Then, the Bade charges of tungsten atoms (*F* and *G*) were +0.12e and +0.18e, as listed in Table 1. Consequently, the tungsten atoms bond (*F*-*G*) in the hydrogen atom-segregated tungsten grain boundary became weaker than that in the clean tungsten grain boundary. This leaded to the theoretical tensile strength of the hydrogen atom-segregated tungsten grain boundary being lower than that of the clean tungsten grain boundary. Therefore, the physical origin for the hydrogen-induced embrittlement was the charge transfer induced by hydrogen in the tungsten grain boundary.

4 Conclusions

First-principles calculations have been employed to determine the theoretical tensile strength of the tungsten grain boundary with the hydrogen atom segregation. The tensile strength of the clean tungsten grain boundary was 36.23 GPa, which was 22% lower than that of the bulk tungsten along the same direction. With the hydrogen atom segregation, the tensile strength of the tungsten grain boundary decreased to 32.85 GPa, about 9% lower than that of the clean tungsten grain boundary. The Griffith fracture energy of the hydrogen atom-segregated grain boundary was 2.48 J/m^2, which was lower than that of the clean grain boundary by about 4%. The difference of solution energies for the hydrogen atom at the grain boundary and the fracture free surface was calculated to be −0.08 eV, which was negative, indicating that hydrogen was a grain boundary embrittler according to the Rice-Wang thermodynamic theory. The Bader charge analysis suggested that the physical origin for hydrogen-induced embrittlement was the charge transfer induced by hydrogen in the tungsten grain boundary.

Acknowledgements

This research is supported by the National Magnetic Confinement Fusion Program through Grant No. 2009GB106003. Hong-BO ZHOU acknowledges the support of the Innovation Foundation of BUAA for PhD Graduates.

References

[1] LEE H T, HAASZ A A, DAVIS J W, et al. Hydrogen and helium trapping in tungsten under single and sequential irradiations [J]. J Nucl Mater, 2007, 360: 196−207.

[2] NAGATA S, TAKAHIRO K. Deuterium retention in tungsten and molybdenum [J]. J Nucl Mater, 2000, 283: 1038−1042.

[3] LIU Y L, ZHANG Y, LUO G N, et al. Structure, stability and diffusion of hydrogen in tungsten: A first-principles study [J]. J Nucl Mater, 2009, 390: 1032−1034.

[4] LIU Y L, ZHANG Y, ZHOU H B, et al. Vacancy trapping mechanism for hydrogen bubble formation in metal [J]. Phys Rev B, 2009, 79: 172103.

[5] ZHOU H B, LIU Y L, ZHANG Y, et al. Investigating behaviors of hydrogen in a tungsten grain boundary by first principles: From dissolution and diffusion to a trapping mechanism [J]. Nucl Fusion, 2010, 50: 025016.

[6] ZHOU H B, LIU Y L, SHUO J, et al. Towards suppressing H blistering by investigating the physical origin of the H–He interaction in W [J]. Nucl Fusion, 2010, 50: 115010.

[7] LI W Y, ZHANG Y, ZHOU H B, et al. Stress effects on stability and diffusion of H in W: A first-principles study [J]. Nucl Instrum

Methods Phys Res B, 2011, 269: 1731−1734.

[8] ZAJEC B, NEMANIC V, RUSET C. Hydrogen diffusive transport parameters in W coating for fusion applications [J]. J Nucl Mater, 2011, 412: 116−122.

[9] AOKI K, IZUMI O. Improvement in room temperature ductility of the L1//2 type intermetallic compound Ni//3Al by boron addition [J]. J Japan Inst Metals, 1979, 43: 1190−1196.

[10] LEJCEK P, HOFMANN S. Thermodynamics and structural aspects of grain boundary segregation [J]. Crit Rev Sol State Mater Sci, 1995, 20: 1−85.

[11] WETZEL J T, MACHLIN E S. Computer simulation of solute segregation to a $\Sigma = 5$ tilt boundary in Au, Cu and Ni [J]. Surf Sci, 1984, 144: 124−152.

[12] LU G H, ZHANG Y, DENG S, et al. Origin of intergranular embrittlement of Al alloys induced by Na and Ca segregation: Grain boundary weakening [J]. Phys Rev B, 2006, 73: 224115.

[13] ZHANG Y, LU G H, DENG S, et al. Weakening of an aluminum grain boundary induced by sulfur segregation: A first-principles computational tensile test [J]. Phys Rev B, 2007, 75: 174101.

[14] ZHANG L, SHU X L, JIN S, et al. First-principles study of He effects in a bcc Fe grain boundary: site preference, segregation and theoretical tensile strength [J]. J Phys Condens Matter, 2010, 22: 375401.

[15] HAASZ A A, POON M, DAVIS J W. The effect of ion damage on deuterium trapping in tungsten [J]. J Nucl Mater, 1999, 266: 520−525.

[16] CAUSEY R A. Hydrogen isotope retention and recycling in fusion reactor plasma-facing components [J]. J Nucl Mater, 2002, 300: 91−117.

[17] SHIMADA T, KURISHITA H, UEDA Y, et al. Blister formation in tungsten by hydrogen and carbon mixed ion beam irradiation [J]. J Nucl Mater, 2003, 313: 204−208.

[18] FUNABIKI T, SHIMADA T, UEDA Y, et al. Effect of tungsten microstructure on blister formation by hydrogen and carbon mixed ion beam irradiation [J]. J Nucl Mater, 2004, 329: 780−784.

[19] UEDA Y, FUNABIKI T, SHIMADA T, et al. Hydrogen blister formation and cracking behavior for various tungsten materials [J]. J Nucl Mater, 2005, 337: 1010−1014.

[20] KOHYAMA M. Tensile strength and fracture of a tilt grain boundary in cubic SiC: A first-principles study [J]. Phil Mag Lett, 1999, 79: 659−672.

[21] KOHYAMA M. Ab initio study of the tensile Polar strength and fracture of coincidence tilt boundaries in cubic SiC: interfaces of the {122} Σ=9 boundary [J]. Phys Rev B, 2002, 65: 184107.

[22] ZHANG Y, LU G H, HU X, et al. First-principles computational tensile test on a Na-segregated Al grain boundary with an Si additive and an intergranular embrittlement suppression mechanism [J]. J Phys Condens Matter, 2007, 19: 456225.

[23] KRESSE G, HAFNER J. Ab initio molecular dynamics for liquid metals [J]. Phys Rev B, 1993, 47: 558−561.

[24] KRESSE G, FURTHMÜLLER J. Efficient iterative schemes for ab initio total-energy calculations using a plane-wave basis set [J]. Phys Rev B, 1996, 54: 11169−11186.

[25] PERDEW J P, WANG Y. Accurate and simple analytic representation of the electron-gas correlation energy[J]. Phys Rev B, 1992, 45: 13244−13249.

[26] BLOCHL P E. Projector augmented-wave method [J]. Phys Rev B, 1994, 50: 17953−17959.

[27] BARBOUR J P, CHARBONNIER F M, DOLAN W W, et al. Determination of the surface tension and surface migration constants for tungsten [J]. Phys Rev, 1960, 117: 1452−1459.

[28] MONKHORST H J, PACK J D. Special points for Brillouin-zone integrations [J]. Phys Rev B, 1976, 13: 5188−5192.

[29] NIELSEN O H, MARTIN R M. Quantum-mechanical theory of stress and force [J]. Phys Rev B, 1985, 32: 3780−3791.

[30] LU G H, DENG S, WANG T, et al. Theoretical tensile strength of an Al grain boundary [J]. Phys Rev B, 2004, 69: 134106.

[31] RICE J R, WANG J S. Embrittlement of interfaces by solute segregation [J]. Mater Sci Eng A, 1989, 107: 23−40.

[32] BADER R W F, Atoms in molecules: A quantum theory [M]. Oxford: Oxford University Press, 1990.

[33] HENKELMAN G, ARNALDSSON A, JONSSON H. A fast and robust algorithm for Bader decomposition of charge density [J]. Comput Mater Sci, 2006, 36: 354−360.